PERGAMON

Radiation Physics and Chemistry 53 (1998) 99–105

Radiation Physics and Chemistry

Modifications of radiation detection response of PADC track detectors by photons

D. Sinha, K.K. Dwivedi *

Department of Chemistry, North-Eastern Hill University, Shillong 793 003, India

Received 21 August 1997; accepted 11 November 1997

Abstract

Photon induced modifications in polyalyldiglycol carbonate (PADC) track detectors have been studied in the dose range of 10^1–10^6 Gy. It was found that some of the properties like bulk-etch rate, track-etch rate got enhanced at the dose of 10^6 Gy. Activation energy for bulk-etching has been determined for different gamma doses. In order to correlate the high etch rate with the chemical modifications, UV–Vis, IR and ESR studies were carried out. These studies clearly give the indication that radiation damage results into radical formation through bond cleavage. TGA study was performed for understanding the thermal resistance of this detector. The results are presented and discussed.

Keywords: Bulk-etch rate; PADC; ^{60}Co; ^{252}Cf; Gamma dose; Activation energy

1. Introduction

Chemical modifications observed in irradiated polymeric materials have imparted the initial motivation for studying their impact on track registration properties of a sensitive detector. In polymeric track detectors, only those charged particles with linear energy transfer (LET) above a critical values can create distinct etchable tracks. Atomic radiations such as UV rays and X-rays, nuclear radiations like gamma rays and beta rays are low LET radiations. They mostly affect the physical and chemical properties of the polymeric films. Though they cannot create any tracks but can affect etch rate values of detectors depending upon the absorbed dose (Frank and Benton, 1970). For track detectors exposed to high LET charged particles followed or preceded by low LET radiation exposure, both the bulk-etch rate and track-etch rate are found to vary in accordance with the absorbed doses of low LET radiations (Shweikani et al., 1993; Sinha et al., 1997a). Having a thorough knowledge about these effects is, therefore, necessary when track detectors are used for detecting charged particles in an atmosphere of intense low LET background radiation. Besides, it is useful in evaluating the dosimetric properties of track detectors.

Polyalyldiglycol carbonate (PADC, generally referred as CR-39 in literature) is a class of plastic detectors which has been most widely used for charged particle detection and measurement. It has already been observed that track registration properties are greatly influenced by exposing them to high gamma dose in the case of CR-39 (Frank and Benton, 1970; Khan et al., 1975; Akber et al., 1980; Zamani et al., 1986; Portwood and Henshaw, 1986; Sharma et al., 1991; Sinha et al., 1997a; Abu-Jarad et al., 1997). Study of optical properties as well as variation of transmittance of the detector was carried out by Joseph and Varier (1995). Seeing all these dose dependent variations in physical and chemical properties, we have attempted in this paper to study systematically the effect of different gamma doses (10^1–10^6 Gy) on PADC. Since this particular detector finds usefulness in many of the nuclear experiments with high gamma background, so it is worthwhile to study the effect of

* Corresponding author.

0969-806X/98/$19.00
PII: S0969-806X(98)00013-9

high gamma exposure on its track registration properties. Our main objectives have been to study the dependence of etch rates, activation energy for bulk-etching, variation of absorbance or transmittance on gamma doses. Electron spin resonance (ESR) as well as thermogravimetric analysis (TGA) studies were also carried out for understanding the radical formation and variation of thermal stability caused by gamma radiation.

2. Experimental

2.1. Irradiation of the detectors

The PADC (American Acrylics) detectors (thickness = 650 μm and density = 1.32 g ml^{-1}) were used in this study. The gamma irradiation of these detectors was done by a gamma source of ^{60}Co, having a dose rate of 3 kGy h^{-1}. Two sets of seven samples each of size 2 × 2 cm^2 were prepared. Then, they were washed thoroughly with soap solution and deionised water. The clean samples were dried and used for irradiation. One set of samples was first exposed at normal incidence to alpha and fission fragments from a ^{252}Cf source for about 10 min. The pre-exposed samples together with the unexposed (second) set of samples were then irradiated with various doses of gamma rays (10^1–10^6 Gy). The exposure time varied from 12 s to nearly 14 days in order to deliver the required doses. The errors in doses range from 8% for low dose (10 Gy) to about 1% for high doses. After gamma exposure, the second set was exposed to a ^{252}Cf source. The first and second sets are respectively referred to post-gamma and pre-gamma set. The detectors were cut into small pieces and track study was performed.

2.2. Chemical etching

The detectors were etched in 6 M NaOH solution at different temperatures, viz., 55, 60, 65, 70°C for different time periods. The accuracy in the maintenance of temperature was ±1°C. The diameters of the fission fragment tracks were measured by using Leitz optical microscope. The magnification of the microscope was about 1560 ×. The diameters of nearly 20–25 tracks were measured for each detector to find out the most probable track diameters (in the range between 2.36 and 13.74 μm) and the error involved in the measurement of track diameters was ±0.43 μm. Then, the bulk-etch rates (V_G) were determined by plotting track diameter of fission fragments vs. etching time. Diameters of the alpha particle tracks were also measured and then converted to track-etch rate by using the standard relation proposed by Shweikani et al. (1993).

2.3. Spectroscopic study

UV and VIS spectra were taken by Beckman (DU-650) spectrophotometer. Small pieces of 0.5 × 1.0 cm^2 were put inside a quartz-shell and the absorption spectra were recorded in the range 200–800 nm, keeping air as the reference. The scan speed was 1200 nm min^{-1}. All the spectra were taken in the solid state. Because of the high thickness of this particular detector, no absorption peak was observed. In order to overcome this problem, the samples were ground properly and made into a thin film on a transparency sheet with nujol and the absorption spectra were taken. Before taking the spectra, the backgrounds of the nujol and transparency sheet were taken, so that the resultant spectra does not have any background effect. IR spectra were also not possible to record in the solid state. Because of the larger thickness of the sample, all the characteristic peaks go beyond the saturation point. So in this case, the samples were ground properly with KBr and a thin layer was prepared. Then, the spectra were taken by a Perkin–Elmer (983-IR) spectrophotometer, in the 4000–500 cm^{-1} region. First derivative ESR measurements were done on Varion E-109, X-band spectrometer with 100 kHz field modulation. A 9.6 GHz microwave frequency was used for this instrument. Samples of sizes (0.5 × 0.5) cm^2 each were put inside a quartz tube (one at a time) and the spectra were recorded at room temperature. The instrumental setup for ESR studies were as follows: Field set = 3380 ± 800 Hz, time constant = 0.250 s, scan time = 8 min, amplitude = 0.5 Gauss, receiver gain = 1.25 × 10^5, microwave power = 5 mW. Thermogravimetric studies were performed using a PERKIN-ELMER instrument. For this study, the samples were cut into very small pieces (0.25 × 0.25 cm^2) and then put on a thermobalance. The samples were then heated up to the temperature of around 610°C at a heating rate of 20°C min^{-1}. This heating results in weight loss, which is recorded as a function of temperature in the TGA thermogram.

3. Results and discussions

The detector remained colourless up to the dose of 10^4 Gy. At 10^5 Gy, it became yellow and at a higher dose that is at 10^6 Gy, the detector turned red. This change in colour is attributed to the formation of radicals (colour centres) in the detector matrix. Figs. 1–2 give the bulk-etch rate (V_G) and track-etch rate (V_T) at different doses of gamma radiation, respectively. It

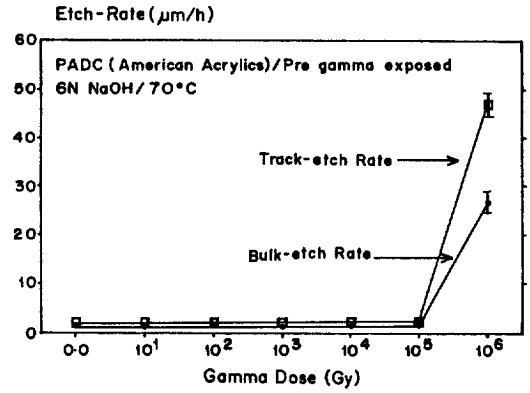

Fig. 1. The effect of pre-gamma exposure on bulk and track-etch rates of PADC etched at 70°C in 6 M NaOH.

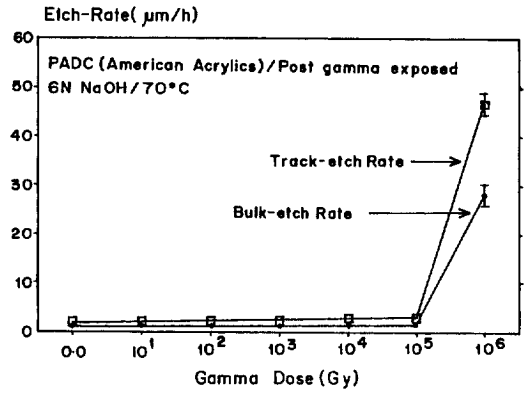

Fig. 2. The effect of post-gamma exposure on bulk and track-etch rates of PADC etched at 70°C in 6 M NaOH.

shows that both V_G and V_T remain almost invariant up to a gamma dose of 10^5 Gy. However, there is a steep increase in both V_G and V_T at a dose of 10^6 Gy. This enhanced response of detector at 10^6 Gy was observed in both the cases of pre- and post-gamma exposure. Similar increase in etch rates at the dose of 10^6 Gy, for PADC (Homalite) was also observed in an earlier work (Sinha et al., 1997a). It was found earlier that post-gamma exposure had higher etch rate values than the pre-gamma exposure. But in the present case there is no significant change in bulk-etch rate as well as in track-etch rate for post-gamma exposed samples.

A possible explanation for the increase in etch-rates at a dose of 10^6 Gy can be attributed to the decrease in the average molecular weight (Fleischer et al., 1975) by scissions of the molecular chains caused by gamma rays (Khan et al., 1975; Zamani and Charalambous, 1981). Tables 1–4 lists the bulk-etch rate and track-etch rate values of the detector at different temperature and for both pre- and post-exposure set.

Table 1
Bulk-etch rate (V_G) in μm h^{-1} for pre-gamma exposed PADC etched in 6 M NaOH

T (°C)	No dose	10^1 Gy	10^2 Gy	10^3 Gy	10^4 Gy	10^5 Gy	10^6 Gy
55	0.35 ± 0.05	0.34 ± 0.05	0.34 ± 0.05	0.38 ± 0.05	0.39 ± 0.05	0.47 ± 0.05	7.70 ± 1.1
60	0.59 ± 0.06	0.58 ± 0.06	0.57 ± 0.06	0.59 ± 0.06	0.73 ± 0.06	0.82 ± 0.06	11.48 ± 1.2
65	0.85 ± 0.10	0.87 ± 0.10	0.88 ± 0.10	0.89 ± 0.10	1.16 ± 0.10	1.22 ± 0.10	18.90 ± 1.3
70	1.15 ± 0.11	1.15 ± 0.11	1.15 ± 0.11	1.22 ± 0.11	1.19 ± 0.11	1.58 ± 0.11	26.95 ± 1.8

Table 2
Bulk-etch rate (V_G) in μm h^{-1} for post-gamma exposed PADC etched in 6 M NaOH

T (°C)	No dose	10^1 Gy	10^2 Gy	10^3 Gy	10^4 Gy	10^5 Gy	10^6 Gy
55	0.35 ± 0.05	0.35 ± 0.05	0.36 ± 0.05	0.38 ± 0.05	0.44 ± 0.05	0.50 ± 0.02	8.15 ± 1.1
60	0.59 ± 0.06	0.59 ± 0.06	0.59 ± 0.06	0.60 ± 0.06	0.82 ± 0.06	0.90 ± 0.06	12.58 ± 1.2
65	0.85 ± 0.10	0.86 ± 0.10	0.86 ± 0.10	0.90 ± 0.10	1.21 ± 0.10	1.35 ± 0.10	21.27 ± 1.3
70	1.15 ± 0.11	1.14 ± 0.11	1.15 ± 0.11	1.15 ± 0.11	1.47 ± 0.11	1.66 ± 0.11	28.04 ± 1.8

Table 3
Track-etch rate (V_T) in μm h^{-1} for pre-gamma exposed PADC etched in 6 M NaOH

T (C)	No dose	10^1 Gy	10^2 Gy	10^3 Gy	10^4 Gy	10^5 Gy	10^6 Gy
55	0.54 ± 0.05	0.53 ± 0.05	0.52 ± 0.05	0.57 ± 0.05	0.55 ± 0.05	0.69 ± 0.05	14.27 ± 1.1
60	0.87 ± 0.06	0.89 ± 0.06	0.88 ± 0.06	0.91 ± 0.06	1.05 ± 0.06	1.26 ± 0.06	19.95 ± 1.2
65	1.11 ± 0.10	1.15 ± 0.10	1.07 ± 0.10	1.09 ± 0.10	1.51 ± 0.10	1.73 ± 0.10	29.29 ± 1.3
70	1.86 ± 0.11	1.86 ± 0.11	1.96 ± 0.11	1.95 ± 0.11	2.17 ± 0.11	2.49 ± 0.11	46.54 ± 1.8

Table 4
Track-etch rate (V_T) in μm h^{-1} for post-gamma exposed PADC etched in 6 M NaOH

T (°C)	No dose	10^1 Gy	10^2 Gy	10^3 Gy	10^4 Gy	10^5 Gy	10^6 Gy
55	0.54 ± 0.05	0.54 ± 0.05	0.54 ± 0.05	0.55 ± 0.05	0.72 ± 0.05	0.76 ± 0.05	14.32 ± 1.1
60	0.87 ± 0.06	0.90 ± 0.06	0.91 ± 0.06	0.89 ± 0.06	1.22 ± 0.06	1.36 ± 0.06	20.18 ± 1.2
65	1.11 ± 0.10	1.12 ± 0.10	1.12 ± 0.10	1.23 ± 0.10	1.55 ± 0.10	1.87 ± 0.10	29.45 ± 1.3
70	1.86 ± 0.11	1.85 ± 0.11	1.99 ± 0.11	1.99 ± 0.11	2.77 ± 0.11	2.90 ± 0.11	46.70 ± 1.8

Table 5
Activation energy (Q) in kJ mol^{-1} for bulk-etching of PADC detector at different gamma doses

Gamma dose	No dose	10^1 Gy	10^2 Gy	10^3 Gy	10^4 Gy	10^5 Gy	10^6 Gy
Pre-exposure	63.9 ± 4.3	65.6 ± 4.6	66.1 ± 3.8	67.9 ± 4.6	65.4 ± 4.6	67.1 ± 3.6	69.3 ± 4.6
Post-exposure	63.9 ± 4.3	63.3 ± 4.3	62.3 ± 4.3	61.3 ± 4.3	63.5 ± 4.3	64.1 ± 4.3	68.5 ± 4.6

The activation energy (Q) for bulk-etching have been determined by plotting log V_G against the reciprocal of the etching temperature (in absolute units) for different doses and are listed in Table 5. The activation energy for the pristine material is found around 63.9 ± 4.3 kJ mol^{-1} which is much lower than the activation energy (117.1 ± 4.5 kJ mol^{-1}) found for another type of PADC detector (Sinha et al., 1997a) manufactured by Homalite. It was also observed in our earlier work (Sinha et al., 1997a,b) for Triafol-BN and PADC (Homalite) detectors that the activation energy remains the same, even though the etch-rate increases after exposure to higher gamma doses. In the present case, similar results have been observed. The constancy in the values of activation energy (within experimental errors) in spite of an increase in bulk-etch rate is attributed to an increase in the rate constant (A) value in the Arrhenius equation. The activation energy remains unaltered under different doses of gamma radiation which suggests that the damage of the bulk material has no significant influence on this parameter.

Fig. 3 shows the UV–Vis absorption spectra of PADC exposed to different doses of gamma radiation. Though the absorption spectra does not give any absorption peak, it is interesting to observe that above the dose of 10^3 Gy, absorption pattern changes with increasing gamma dose. Moreover, with increasing gamma dose the absorption shifts towards higher wave length. The UV–Vis spectra taken from the powdered material have not revealed any specific chemical change as the peak positions are not altered by exposing the samples to different doses of gamma radiation.

In order to assess the scope of this study in dosimetric applications, transmittance were plotted at different wavelengths for samples exposed to different gamma doses. Fig. 4 shows the plots of transmittance as function of gamma doses. From these plots, one may estimate the radiation dose by measuring the transmittance.

The information about any specific bond cleavage could not be derived from the IR spectra of PADC

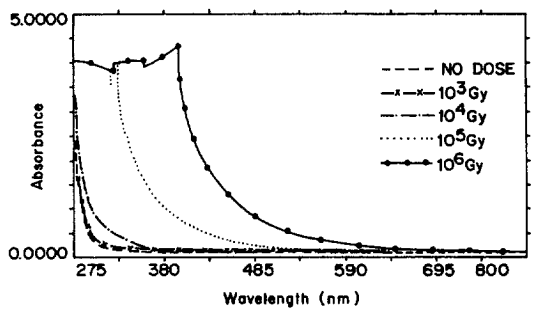

Fig. 3. UV and Vis absorption spectra of PADC detector exposed to different doses of gamma rays.

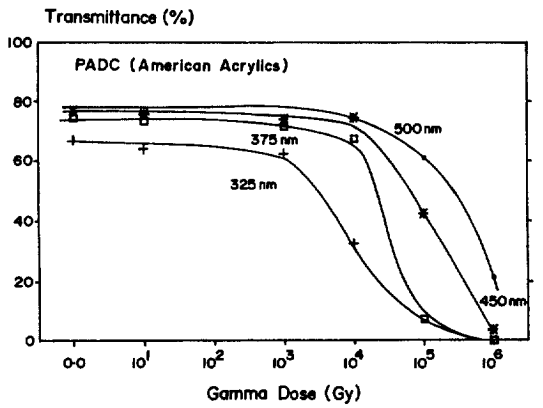

Fig. 4. Dose dependence transmission (%) spectra of gamma irradiated PADC detector.

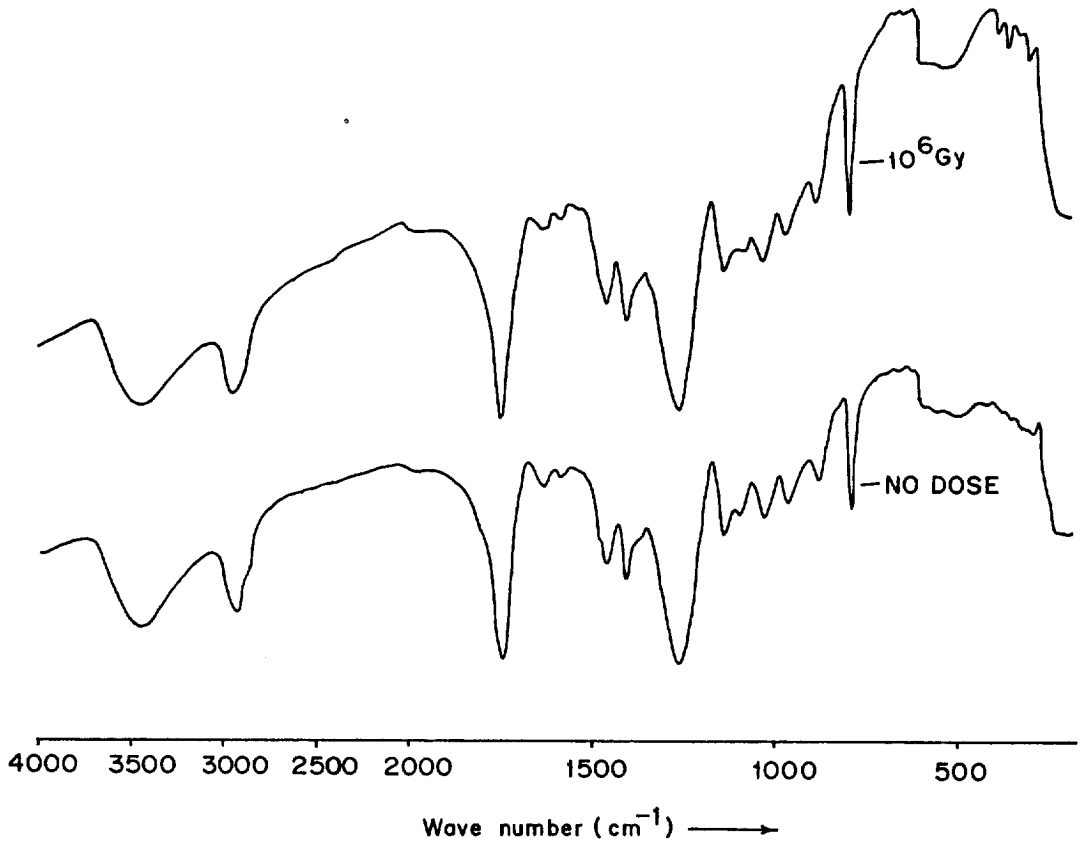

Fig. 5. IR spectra of gamma irradiated PADC detector.

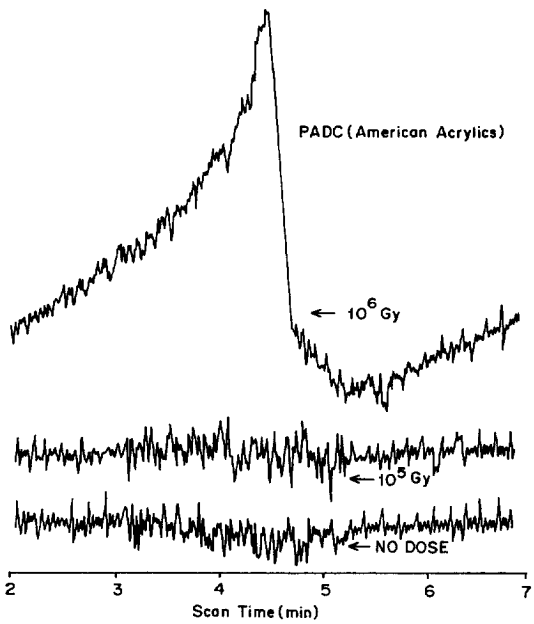

Fig. 6. ESR spectra of pristine and irradiated PADC in which the presence of oxygen radical is indicated by a broad signal at a dose of 10^6 Gy.

exposed to different doses. Fig. 5 contains IR spectra for pristine and gamma irradiated (10^6 Gy) PADC samples. Some of the characteristics peaks observed in IR spectra are $\nu_{C-H} = 2954$ cm^{-1}, $\nu_{C=O} = 1742$ cm^{-1}, $\nu_{C-O} = 1260$ cm^{-1}, $\nu_{C-C} = 1136$ cm^{-1} and $\delta_{-(CH2)-} = 788$ cm^{-1} (bending vibrations of the group $-(CH_2)_n-$).

ESR study gives a clear picture about the bond cleavage. The track study has indicated that the increase in etch rate is due to the cleavage of polymeric chain, but there is no supporting evidence found from IR and UV–Vis study. The ESR study shows that up to the dose of 10^5 Gy, no signal corresponding to radical formation is found. This means the intensity of scissioning (below 10^5 Gy) is low and is not reflected as ESR signal. But at the dose of 10^6 Gy, one gets a clear broad radical signal as shown in Fig. 6. This sort of broad radical signal is the characteristic of oxygen radical. It can be possible only if polyalyl chain breaks and forms the radicals.

PADC polymer network consists of polyalyl chains joined by diethyleneglycol links which must be hit by radiation. The possible route of gamma induced scission of PADC polymer chain is as follows

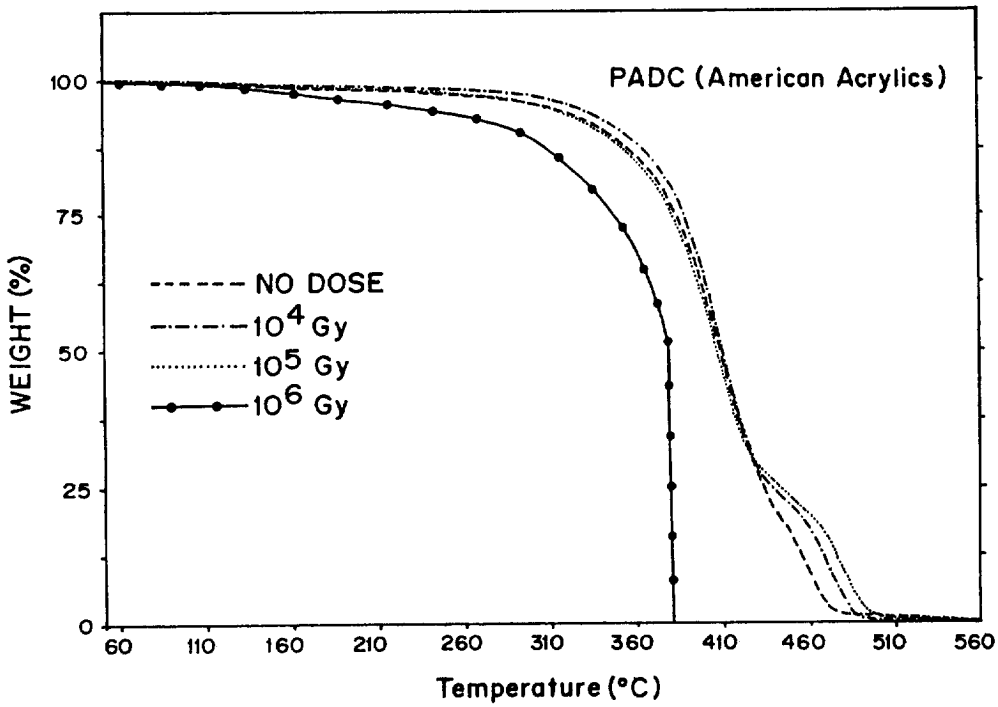

Fig. 7. A thermogram of pristine and gamma irradiated PADC. The nature of curve indicates a two-step process of thermal decomposition.

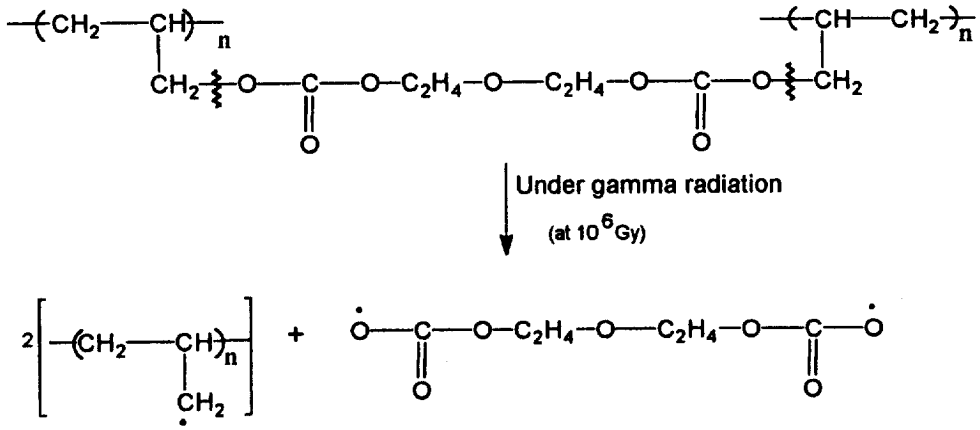

Two of the radicals with carbon end thus formed may combine with each other and re-establish the polymeric linkage. That is why we get the signal for the oxygen radical only.

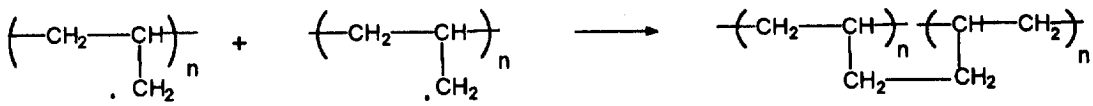

Thermogravimetric analysis of pristine and gamma irradiated (up to 10^5 Gy) PADC polymer shows double step decomposition pattern. The first step of decomposition starts around 300°C and finishes around 430°C. In this temperature range about 70% of the total weight decomposes. The thermal stability curves show identical response up to 10^5 Gy in first step. The second step of decomposition starts at

430°C and continues up to around 475–485°C as shown in Fig. 7. From the second step decomposition curves, one observes that the material gains some thermal stability up to 10^5 Gy. But at the dose of 10^6 Gy, only single step decomposition was observed. In this case the weight loss starts around 260°C and 100% weight loss takes place around 380°C. Up to a dosage of 10^5 Gy, the detector was stable till a temperature range of 475–485°C. But when the dose becomes 10^6 Gy, the thermal resistance comes down and the detector decomposes at lower temperature.

4. Conclusions

On the basis of the present results and above discussion, we conclude that:

(a) Up to 10^5 Gy, the intensity of bond scissioning or cross-linking is too low to show up as a macroscopic signal.

(b) The bonds joining polyalyl chains with diethyleneglycol have been possibly attacked by gamma rays to produce following radicals:

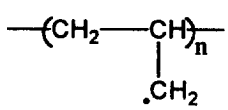

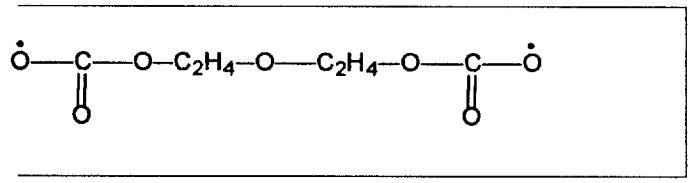

(c) This bond cleavage reduces the average molecular weight and consequently the etch-rate increases.

(d) Although the etch-rate increases with gamma dose, there is no significant change in the etch-rate values of PADC for pre- and post- mode of gamma exposure.

(e) Although the bulk-etch rate increases at higher doses, but the activation energy for bulk-etching does not change significantly.

(f) The dosimetric applications of this polymer have shown some potential for gamma doses between 10^3–10^6 Gy.

Further work is in progress to generate Tauc's plot for determining the influence of different gamma doses on the magnitude of optical band gap of the material and the size of carbon clusters formed due to irradiations.

Acknowledgements

One of the authors D. Sinha is grateful to CSIR, New Delhi, for the financial assistance in the form of Senior Research Fellowship. We are thankful to Dr. V.G. Dedgaonkar, Pune University, for the gamma exposure of the detectors.

References

Abu-Jarad, F., Hala, A.M., Farhat, M., Islam, M., 1997. Effect of high gamma dose on the CR-39 properties. Radiat. Meas., 28, 111.

Akber, R.A., Nadeem, K., Majid, C.A., Hussain, A., Zaman, N., Chaudhary, M.A., Khan, H.A., 1980. Studies of structural changes produced by high doses of gamma rays in some plastic track detectors. Nucl. Instr. Meth. 173, 217.

Fleischer, R.L., Price, P.B., Walker, R.M., 1975. Nuclear Tracks in Solids: Principles and Applications. University of California Press, Berkeley.

Frank, A.L., Benton, E.V., 1970. Dielectric plastics as high-exposure gamma-ray detectors. Radiat. Effects 2, 269.

Joseph, A., Varier, K.M., 1995. Gamma ray dosimetric studies on CR-39 detector. Indian J. Pure Appl. Phys. 33, 406.

Khan, H.A., Asharf, M.A., Yameen, S., Haroon, M.R., Hussain, A., 1975. The effects of high gamma doses on the response of plastic track detectors. Nucl. Instr. Meth. 127, 105.

Portwood, T., Henshaw, D.L., 1986. The effect of gamma dose on the alpha response of CR-39. Nucl. Tracks 12, 105.

Sharma, S.L., Pal, T., Rao, V.V., Enge, W., 1991. Effect of gamma irradiation on bulk etch rate of CR-39. Nucl. Tracks Radiat. Meas. 18, 385.

Shweikani, R., Durrani, S.A., Tsuruta, T., 1993. Effects of gamma irradiation on the bulk and track etching properties of cellulose nitrate (Daicel 6000) and CR-39 plastics. Nucl. Tracks Radiat. Meas. 22, 153.

Sinha, D., Ghosh, S., Srivastava, A., Dedgaonkar, V.G., Dwivedi, K.K., 1997a. Effect of gamma rays on PADC detectors. Radiat. Meas. 28, 145.

Sinha, D., Sarker, G.K., Ghosh, S., Kulshreshtha, A., Dwivedi, K.K., Fink, D., 1997b. Photon induced modifications in Triafol-TN and Triafol-BN polymeric track detectors, Radiat. Meas. (communicated).

Zamani, M., Charalambous, S., 1981. The response of cellulose nitrate to gamma radiation. Nucl. Tracks 4, 171.

Zamani, M., Sampsonidis, D., Charalambous, S., 1986. Dose rate effects on CR-39 SSNT detector. Nucl. Tracks 12, 125.